Available online at www.sciencedirect.com

ScienceDirect

Procedia Manufacturing 47 (2020) 1264–1269

Procedia MANUFACTURING

www.elsevier.com/locate/procedia

23rd International Conference on Material Forming (ESAFORM 2020)

Strain Rate Effect on the Fracture Behavior of the AA5754 Aluminum Alloy

Maddi Bueno[a], Lander Galdos[a], Eneko Sáenz de Argandoña[a], Matthias Weiss[b], Bernard Rolfe[c], Yanshan Lou[d], Joseba Mendiguren[a,*]

[a]Mondragon Unibertsitatea, 4 Loramendi, 20500 Mondragon Spain
[b]Institute for Frontier Materials, Deakin University, Waurn Ponds, Pigdons Rd., VIC, 3216, Australia
[c]School of Engineering&Information technology, Deakin University, Waurn Ponds, Pigdons Rd., VIC, 3216, Australia
[d]School of Mechanial Engineering, Xi'an Jiaotong University, 28 Xianning West Road, Xi'an, Shaanxi 710049, China

* Corresponding author. Tel.: +34 664 236 243; *E-mail address:* jmendiguren@mondragon.edu

Abstract

Stamping of aluminum alloy is becoming of great interest by the automotive industry in the last years. With the increase in the use of these materials, problems such as die wear, galling and springback, for example, are becoming critical. Among them, the instability of the process to manufacturing-process-windows (holding force pressure windows and drawing speed windows for example) are involving a lot of engineering challenges. As an example, the impact of the use of hydraulic presses against the use of mechanical presses leads to an apparition or solving of fracture problems. Being the drawing speed the main difference between them, numerous effects can be responsible for those differences, e.g. strain rate sensitivity of the plastic behavior, drawing speed sensitivity of the tribological behavior, temperature effect. In that regard, in this work, the strain rate sensitivity of the damage-fracture behavior of the AA5754 material is studied.

Keywords: ductile fracture; aluminum; strain rate

1. Introduction

Stamping is one of the most used manufacturing technologies on the automotive industry, being the later one among the largest mass production industries in the world. It is a well stablished manufacturing process and therefore the maturity of the knowledge is very high. However, the change on trends on the markets, i.e. CO2 regulations, safety regulations, customers perspective has led to the increase of some problems in the last years. It is well known that some of the challenges on the stamping these days are related with the correct prediction of forming strategies in order to avoid the costly try and error method. Among all the phenomena that still nowadays is not well stablished from the numerical production point of view, the most relevant can be the springback, cosmetic defect, behavior under non-proportional paths, galling. All these issues have been magnified with the introduction of the high strength steels on the body in white and the aluminum use trend of the last years.

Particularly, on the case of aluminum panel forming, industry is claiming differences on the forming behavior of the material when increasing the production rate. Typically, in try-out step the parts are drawn slowly paying attention to the details, then, when the production starts, the manufacturing rate is slow in order to get everything working smoothly and then, when possible, the manufacturing rate is increased to the maximum available in order to reduce lead-time. Industry is claiming that the die (or material) do not behave the same at the different stages of the increase of production rate. Sometimes

10.1016/j.promfg.2020.04.212

they have material splits at low speed that disappear once the high speed is ruing and sometimes the other way around.

This effect could be linked to the temperature increase due to the subsequent forming at different speeds, to deflections and inertias of the press, to strain rate sensitivity on the material behavior, etc.

In terms of fracture on aluminum alloys, numerous works have been published in the last years regarding ductile fracture behaviors. Ductile fracture criteria however, does not based on extensively experimental measurement of fracture strains under various loading conditions until fifteen tests were carried out by Bao and Wierzbicki (2004) [1] for AA2024-T351 including compressive upsetting tests, shear, and tension. Xue (2007) [2] first considered the effect of the Lode angle together with pressure on ductile fracture. Bai and Wierzbicki (2008) [3] proposed a fracture model with pressure and Lode dependence.

Lou et al., (2012) [4] first coupled the effect of the maximum shear stress on damage accumulation and proposed a relatively simple ductile fracture criterion based on micro-mechanisms of ductile fracture for nucleation, growth and shear linking-up of voids along the direction of the maximum shear stress. During the last years, this model has been developed as Lou and Huh (2013) [5] realized that the effect of the maximum shear stress on ductile fracture was further correlated with the Lode parameter.

Moreover, Park et al., (2017) [6] and Mu et al., (2018) [7] proposed two different fracture criteria separately to consider the effect of the maximum shear stress and the stress triaxiality on damage. Park et al. (2017) [6] suggested an anisotropic stress triaxiality based on the Hill's 48 criterion. This criterion was extended by Park et al. (2018) [8] with a generalized anisotropic stress triaxiality based on the Yld91 criterion. In addition, Lou and Yoon (2018) [9] a plasticity model and a fracture criterion based on the Drucker function.

Huh et al. (2008) [10], conducted experimental tests, strain rates ranging from 0.003/s to 200/s of four different advanced high strength steels (TRIP600, TRIP800, DP600 and DP800). He concluded that for three of the materials the effect of the strain rate was negligible. In contrast, for the TRIP600 steel, increasing the strain rate also increased the elongation to fracture. Curtze et al. (2009) [11] performed experiments and realized that the elongation to fracture for a DP600 steel and a TRIP700 steel were approximately the same irrespective of the strain rate. Erice eta al. (2018) [12] confirm that the ductility increases in the notched specimens as the loading velocity increases on three advanced high strength steels (DP980, CP980 and CP1180).

As a result, at low speeds the effect of strain rate is negligible for high strength steels, but not for high speeds, the higher is the speed, the greater the elongation to the fracture. The effect of strain rate is not the same for all materials, until today, nobody has analyzed its effect on aluminum AA5754 and is a material that is characterized by having many fracture problems.

Therefore, the main objective of this work is to analyses the influence of the strain rate on the damage behavior prediction. In order to do so, first a benchmark type component has been analyzed in order to establish the characteristic strain rates on a conventional drawing operation. Then, fracture test specimens have been tested at different strain rates in order to analyses if the fracture behavior changes when increasing the speed from try-out scenario to high rate stamping scenario.

2. Material

The AA5754 aluminum alloy has been studied in this work. This material grade is one of the most widely used aluminums in the automotive industry nowadays. Figure 1 shows the grain distribution of the analyzed material under the EBSD detector of the SEM microscope.

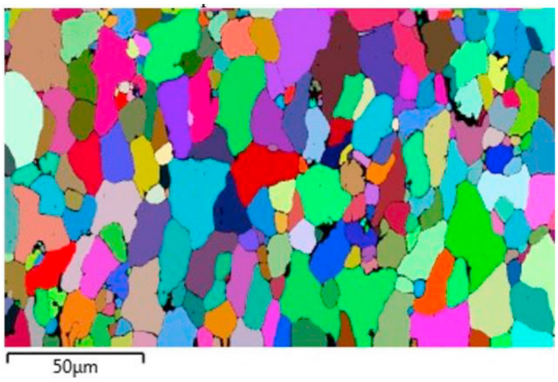

Fig. 1. Grain distribution of the studied AA5754 (EBSD).

Tensile test every 15º to the rolling direction were performed in order to characterize the potential anisotropy of the material. From those tests, the yield stress (Rp_{02}) and the anisotropy values (r-values) were calculated by the standard post processing of GOM Aramis.

Table 1 shows the yield stress distribution for every 15º to the rolling direction while Table 2 shows the r-value distribution for the same samples. When referred to deviation is the standard deviation.

Table 1. Yield stress values under different directions to the rolling direction. Values in MPa.

	0º	15º	30º	45º	60º	75º	90º
Averaged	127	125	122	123	123	127	124
Deviation	1.8	2.8	1.6	2.6	1.4	1.3	1.3

From the values of Table 1 can be denoted that the material does not show a critical anisotropy in terms of initial yield stress. Where the average yielding point is around the 125 MPa ±3 MPa.

Table 2. Anisotropic coefficient values under different directions to the rolling direction.

	0º	15º	30º	45º	60º	75º	90º
Averaged	0.723	0.696	0.793	0.725	0.717	0.728	0.738
Dev. $\cdot 10^{-3}$	2.3	3.6	7.6	4.4	3.7	2.3	3.4

The r-value distribution shown in Table 2 also follows the same trend in where the values are around the 0.7 value without too much differences between direction to the rolling direction.

During the study, samples at the rolling direction (RD), transverse to the rolling direction (TD) and to 45 ° to the rolling direction (45D) were studied. However, for the sake of simplicity, only the discussion of the 45D samples will be shown in the following sections.

3. Analysis framework

Considering that the objective of the work is to analyze the impact of the stamping speed on the fracture behavior of the material, a specific automotive component has been used in order to able to stablish the characteristic strain rates under different stamping scenarios.

As shown in Fig. 2, the drawing step of a wheel arch has been used as a benchmark in this study. This component is characterized by a high drawing depth and therefore high quantity of deformation and material flow into the die cavity.

In Fig. 2 the draw in distribution of the component with the thickness distribution is shown. Due to confidentiality issues, the central part of the drawing is blurry. However, the main point that is that draw-ins of around 100 mm can be found in this component.

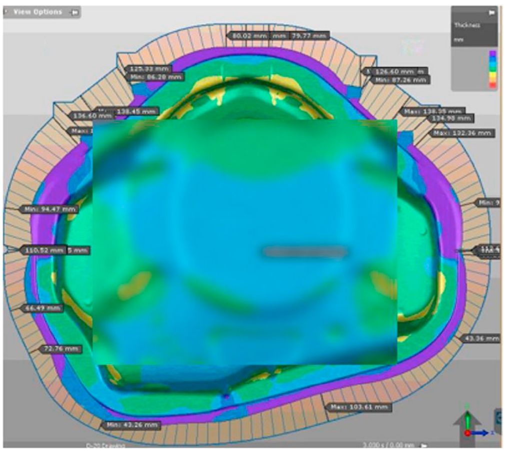

Fig. 2. Wheel arch drawing step in where the drawing of the material is shown together with the thickness distribution.

Using this benchmark, three different case scenarios have been assumed. First, the try out case in where the ram of the press is moved down step by step and when is in continuous it is usually at lower speed. This task is usually performed in hydraulic pressed.

Next, the second case is a low speed forming, usually consistent with the drawing speed in a hydraulic press line. Then, the third case is the high-speed mechanical press line forming in where high process cadency is achieved.

Table 3 summarizes the strain rate range in where each stamping case is located.

Table 3. Strain rate limits for each case study.

Stamping speed	Strain rate
Try out	$3 \cdot 10^{-3}\ s^{-1}$
Low speed production	$2 \cdot 10^{-2}\ s^{-1}$
High speed production	$3\ s^{-1}$

The try out step can have strain rates characteristics of quasi-static range. Of course, during the drawing each point of the material will follow a different strain rate, however the big picture is shown in Table 3.

The higher strain rate achieved during the fast forming can be assumed to be in the range of the $3\ s^{-1}$. Therefore, those three ranges were taken in this study aiming to cover the whole range of action of deformation of the material under different conditions.

4. Methodology

Among the different experimental strategies that can be followed to characterize the fracture behavior of a material, in this work the tensile test-based fracture analysis has been used.

The main idea behind this test methodology is to create sample geometries that lead to different triaxialities (and therefore Lode angle under plane stress assumption) when uniaxiality stretched in a conventional tensile test machine.

In this paper only two examples are going to be analyzed. On the one hand, the notched sample (N). The notched sample geometry shown in Fig. 3a is a dog bone specimen with a reduced calibrated length or what is the same a flat strip with two semi-holes in order to create a stress concentration on the area. The aim of this geometry is to generate a stress sate close to the uniaxial triaxiality of 1/3.

The second geometry on the other hand, is the shear sample (S) and the objective of the geometry is to obtain a pure shear stress state in the center of the specimen.

The geometries used in this study follow the proposal of Dr. Lou and it is described in Fig. 3.

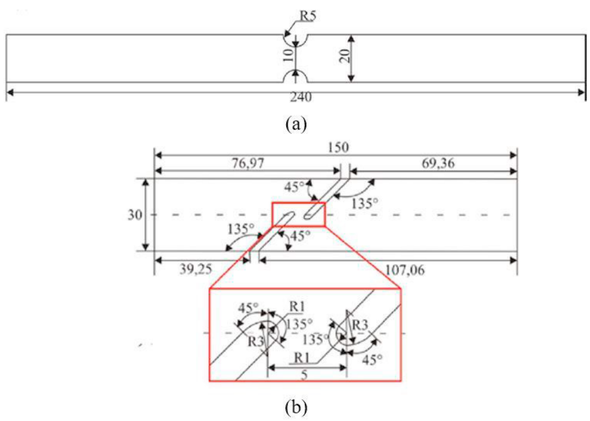

Fig. 3. Fracture specimen geometry; a) notched sample (N) and b) shear sample (S).

It must be noted that each sample require a different test speed (taking as a test speed the velocity of the tensile test machine) in order to achieve the same strain rate. As due to the sample geometry, moving the tensile machine at the same speed different strain rates will be obtained on each sample.

That is why, after some preliminary testing the final machine speed were defined (based on trivial calculations and trial error process) in order to obtain the fracture at the desired strain rates (shown in Table 3).

Every test was monitored in different ways. On one hand, signals from the tensile machine were taken, acquiring the force data from the load force sensor and the stretching of the sample with an extensometer with initial length of 50 mm (this signal will be referred later as displacement). On the other hand, GOM Aramis system was used on the surface of the sample in order to evaluate the full field method and in order to have snapshots of the surface integrity of the sample and be able to evaluate not only the fracture point but also the fracture behavior.

Figure 4 shows the difference between different fracture behaviors in a hole type sample (this sample geometry was not shown in this paper, but it is a good example to explain the fracture behavior concept).

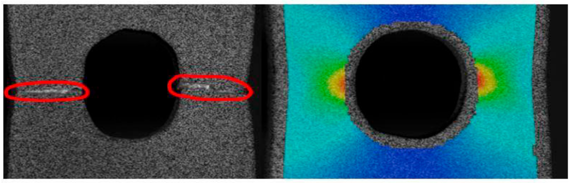

(a)

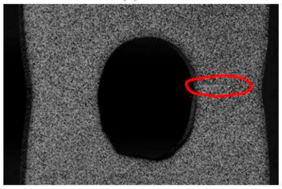

(b)

Fig. 4. Fracture behavior analysis; a) symmetric strain concentration and fracture and b) local fracture stated on the edge of the sample.

Every fracture sample is designed to generate stress concertation of some short and to force the fracture under some specific stress state (triaxiality and lode angle). However, in some cases due to specimen misalignments or edge quality it can happened that the fracture initiating is no under the correct conditions. This effect is highlighted on Fig. 4. On Fig.4a asymmetric strain distribution is observed and the fracture simultaneously occurs in both necks. However, on Fig.4b it can be seen how the fracture is localized only on one part of the geometry and therefore out of the desired area.

By using this observation technique, the undesired fracture behaviour samples were neglected from the study.

Figure 5 shows the strain distribution on the shear sample in where the whole strain concertation is happening in the neck of the geometry. Other studies have proven that the analyzed geometry does not lead to pure shear stress state and further analysis will be necessary in order to stablish the existing stress-strain state during the fracture phase.

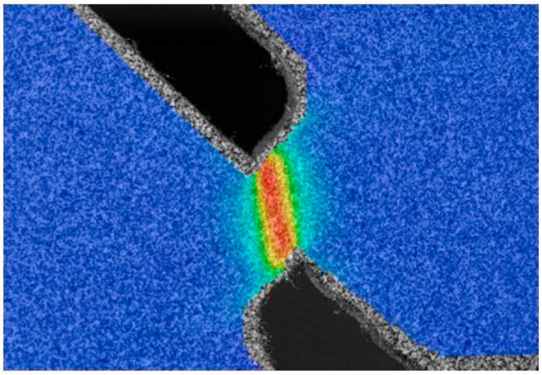

Fig. 5. Shear sample strain distribution during the test.

Five samples were tested under different condition, if in any of the samples an inadequate fracture pattern was observed (e.g. Fig. 4b) a new sample was tested until five adequate fracture samples were obtained. Then, from those results, the displacement averaged value and the standard deviation were analysed.

However, another source of uncertainty that must be considered is the image-to-image uncertainty. Figure 6 schematically shows that uncertainty.

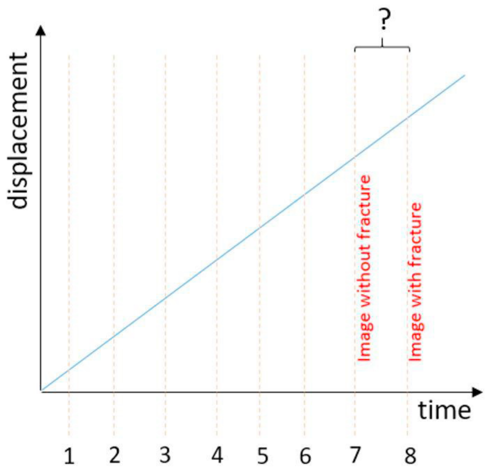

Fig. 6. Image to image uncertainty.

As previously introduced, every test is recorded with GOM Aramis system under the maximum acquisition frequency of the standard set up, 15 Hz. The test is performed and after fracture the images are reviewers in order to identify in which one, we can find the fracture. Figure 6 shows the displacement vs time diagram of the extensometer movement. Being the movement of the machine of a continuous nature only discrete information at specific points is available, at points 1, 2, 3…

Therefore, if in the image 8 the fracture is observed and is not in the image 7, which means that somewhere between both images the fracture has occur. However, it will not be known at what point. Therefore, the uncertainty of image-to-image distance must be added to the raw data experimental as "error" or unknown. This is especially important for the high-speed test configuration in where using the 15 Hz of acquisition higher displacement uncertainty is found between two images.

This error is directly related with the machine velocity and the acquisition frame-rate and it can be critical for high speed testing. In the framework of this work and in view of the obtained uncertainty ranges, it was not necessary to use a high-speed camera, even if this will reduce the image-to-image uncertainty, as the uncertainty was falling on the sample to sample scatter.

5. Results and discussion

Following the above presented methodology, notched (N) and shear (S) fracture samples at 45D were tested under the different test speeds in order to obtain the strain rate ranges shown in Table 3. For the sake of simplicity only result of displacement will be shown in this section.

After the proper analyzing of each fracture pattern, uncertainty and sample-to-sample scatter, the average value of the displacement to fracture was evaluated for each case.

Figure 7 shows the displacement to fracture values for the notched samples while Fig. 8 shows the displacements to fracture for the shear samples.

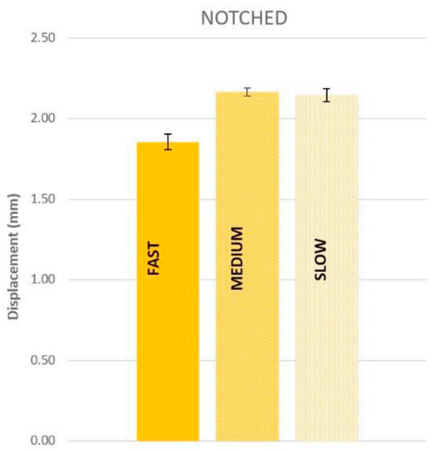

Fig. 7. Notched sample displacement to fracture under different strain rates.

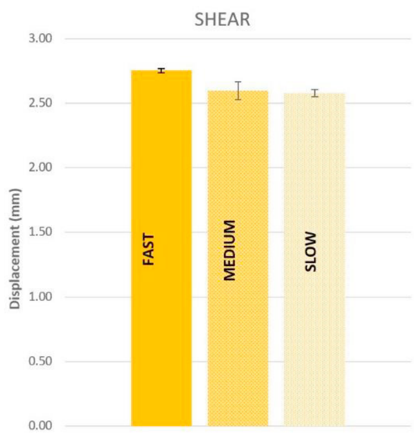

Fig. 8. Shear sample displacement to fracture under different strains.

As from these results can be observed, even considering the uncertainty and the scatter between samples, a marked difference can be seen between the high strain rate (high speed production) and the medium and low (low speed production and try out). On the notched sample, the high strain rate sample has less displacement to fracture while the contrary occurs on the shear geometry. This will suggest an increase of formability on the shear dominated areas and a reduction in the tensile dominated areas when increasing the manufacturing rate in a high-speed stamping line (usually mechanical or servo-mechanical press lines). In view of the results, a further study will be necessary in the high strain rate range as the 10^{-2} s^{-1} and 1^{-3} s^{-1} seems to respond to the same behaviour.

6. Conclusions

From these preliminary results, it can be seeing that a difference can be found on the fracture behavior of the AA5754 depending on the strain rate and therefore this will influence the component formability behavior between try-out and low speed stamping to high speed stamping productions.

It is still unknown if these differences will be remarkable on the strain based fracture limit diagram. In order to do so, further developments will be necessary.

In addition to that, as presented on the introduction, it is still unknown if the main driving phenomenon of the changes when going from low speed production to high speed production are related with this fracture behavior or something else. Further analysis will be also necessary to clarify this issue.

Acknowledgements

The authors want to acknowledge the financial support of the Spanish Government with the project ALUTOOL funded on the Retos-Colaboración program (RTC-2017-6245-4). In addition to that, the authors want to acknowledge the financial support of the Basque Government with the project MIKROMAK funded on the Elkartek program (KK-218/00081).

References

[1] Bao Y, Wierzbicki T. On fracture locus in the equivalent strain and stress triaxiality space. Int J Mech Sci 2004;46:81-98.

[2] Xue L. Damage accumulation and fracture initiation in uncracked ductile solids subject to triaxial loading. IJSS 2007;44:5163-5181.

[3] Bai Y, Wierzbicki T. A new model of metal plasticity and fracture with pressure and Lode dependence. Int Jour Plasticity 2008;24:1071-1096.

[4] Lou Y, Huh H, Lim S, Pack K. New ductile fracture criterion for prediction of fracture forming limit diagrams of sheet metals. IJSS 2012;49:3605-3615.

[5] Lou Y, Huh H. Extension of a shear-controlled ductile fracture model considering the stress triaxiality and the Lode parameter. IJSS 2013;50:447-455.

[6] Park N, Huh H, Lim SJ, Lou Y, Kang YS, Seo MH. Fracture-based forming limit criteria for anisotropic materials in sheet metal forming. Int J Plast 2017;96:1-35.

[7] Mu L, Zang Y, Wang Y, Long X, Malaquias P, Stemler A. Phenomenological uncoupled ductile fracture model considering different void deformation modes for sheet metal forming. Int J Mech Sci 2018;141:408-423.

[8] Park N, Huh H, Yoon JW. Anisotropic fracture forming limit diagram considering non-directionality of the equi-biaxial fracture strain. IJSS 2018;151:181-194.
[9] Lou Y, Yoon JW. Anisotropic yield function based on stress invariants for BCC and FCC metals and its extension to ductile fracture criterion. Int J of Plas 2018;101:125-155.
[10] Huh H, Kim SB, Song JH, Lim JH. Dynamic tensile characteristics of TRIP-type and DP-type steel sheets for an auto-body. IJ Mech Scie 2008;50:918-931.
[11] Curtze S, Kuokkala VT, Hokka M, Peura P. Deformation behavior of TRIP and DP steels in tension at different temperatures over a wide range of strain rates. Mat Scie and Eng A 2009;507:124-131.
[12] Erice B, Roth CC, Mohr D. Stress-state and strain-rate dependent ductile fracture of dual and complex phase steel. Mech Mat 2018;116:11-32.